# REPORT DOCUMENTATION PAGE

*Form Approved*
*OMB No. 0704-0188*

Public reporting burden for this collection of information is estimated to average 1 hour per response, including the time for reviewing instructions, searching existing data sources, gathering and maintaining the data needed, and completing and reviewing this collection of information. Send comments regarding this burden estimate or any other aspect of this collection of information, including suggestions for reducing this burden to Department of Defense, Washington Headquarters Services, Directorate for Information Operations and Reports (0704-0188), 1215 Jefferson Davis Highway, Suite 1204, Arlington, VA 22202-4302. Respondents should be aware that notwithstanding any other provision of law, no person shall be subject to any penalty for failing to comply with a collection of information if it does not display a currently valid OMB control number. **PLEASE DO NOT RETURN YOUR FORM TO THE ABOVE ADDRESS.**

| 1. REPORT DATE *(DD-MM-YYYY)* | 2. REPORT TYPE | 3. DATES COVERED *(From - To)* |
|---|---|---|
| 31/12/2016 | Performance/Technical Report (Quarterly) | 10/01/16 – 12/31/16 |

**4. TITLE AND SUBTITLE**
A Hybrid Approach to Composite Damage and Failure Analysis Combining Synergistic Damage Mechanics and Peridynamics

**5a. CONTRACT NUMBER**

**5b. GRANT NUMBER**
N00014-16-1-2173

**5c. PROGRAM ELEMENT NUMBER**

**6. AUTHOR(S)**
Dr. Ramesh Talreja

**5d. PROJECT NUMBER**

**5e. TASK NUMBER**

**5f. WORK UNIT NUMBER**

**7. PERFORMING ORGANIZATION NAME(S) AND ADDRESS(ES)**
Texas A&M Engineering Experiment Station (TEES)
400 Harvey Mitchell Parkway, Suite 300
College Station, Texas 77845

**8. PERFORMING ORGANIZATION REPORT NUMBER**
M1601473 / 505170-00001/2

**9. SPONSORING / MONITORING AGENCY NAME(S) AND ADDRESS(ES)**
Office of Naval Research
875 N. Randolph Street, Suite 1425
Arlington, VA 22203-1995

**10. SPONSOR/MONITOR'S ACRONYM(S)**
ONR

**11. SPONSOR/MONITOR'S REPORT NUMBER(S)**

**12. DISTRIBUTION / AVAILABILITY STATEMENT**
unlimited

**13. SUPPLEMENTARY NOTES**

**14. ABSTRACT**

The work performed in the reporting period has been focused on continuation of Task 1.1 and Task 2.2 described in the project proposal. The activities related to Task 1.1 are inclusion of voids in a computational micromechanics failure analysis of a representative volume element containing disordered fiber distributions. Procedures have been developed to simulate occurrence of voids of various sizes within the volume of the composite. Effect of the voids on the initiation of failure has been analyzed. The activities related to Task 2.2 cover the estimation of surface effects and effects at material interfaces in peridynamic models of composites.

**15. SUBJECT TERMS**
Computational micormechanics; Cavitational induced cracking; Peridynamics; Porous media

| 16. SECURITY CLASSIFICATION OF: | | | 17. LIMITATION OF ABSTRACT | 18. NUMBER OF PAGES | 19a. NAME OF RESPONSIBLE PERSON |
|---|---|---|---|---|---|
| a. REPORT | b. ABSTRACT | c. THIS PAGE | | | William Nickerson |
| U | U | U | SAR | 6 | 19b. TELEPHONE NUMBER *(include area code)* 703-696-8485 |

**Standard Form 298 (Rev. 8-98)**
**Prescribed by ANSI Std. Z39.18**

**Quarterly Progress Report, October 1 – December 31, 2016**

# A Hybrid Approach to Composite Damage and Failure Analysis Combining Synergistic Damage Mechanics and Peridynamics

Award Number N00014-16-1-2173

DOD – NAVY – Office of Naval Research

PI: Ramesh Talreja
Co-PI: Florin Bobaru

Executive Summary

*The work performed in the reporting period has been focused on continuation of Task 1.1 and Task 2.2 described in the project proposal. The activities related to Task 1.1 are inclusion of voids in a computational micromechanics failure analysis of a representative volume element containing disordered fiber distributions. Procedures have been developed to simulate occurrence of voids of various sizes within the volume of the composite. Effect of the voids on the initiation of failure has been analyzed. The activities related to Task 2.2 cover the estimation of surface effects and effects at material interfaces in peridynamic models of composites.*

## Task 1.1 Micro-level crack initiation

### Background and motivation

In most manufacturing processes for polymer matrix composites (PMCs) one starts with dry bundles of fibers. On resin infusion, the initially closed-pack fibers are spread out to the extent dictated by the intended fiber volume fraction. Whether the end product is a pre-impregnated layer, or a thick part produced by resin transfer molding (RTM), the configuration in which the fibers finally appear is far from uniform. The final nonuniform distribution of fibers consists of clustered fiber regions and resin pockets. The initiation of failure due to fiber clustering was reported in the Third Quarterly Report. In this reporting period, the presence of voids in the matrix between the fibers has been studied closely. The following results describe the progress made so far.

### Approach and Results

A novel procedure has been devised to create nonuniform fiber distributions by perturbing the initial dry fiber bundle. That procedure was reported in the last quarterly report. The results of the failure analysis of a representative volume element (RVE) thus

simulating a sample of the composite showed that for a given fiber volume fraction in a composite, a more clustered region of fibers (i.e. for smaller range of variation of the radial distance r), initiated debonding earlier (at lower applied strain). Table 1.1, which was previously reported showed that as the fiber clustering increased, i.e. as the radial variation decreased, the debonding occurred sooner, i.e., at lower applied strain. As the fibers are spread out more, the debonding becomes less likely. Note that at the largest radial variation range, ±0.5r, not all realizations produced dilatation induced debonding, and a higher strain had to be applied to get debonding in the realizations that showed this failure.

| Sl No | Radial variation | Rotational Variation (degrees) | No of Realizations | No of Realizations showing dilatational failure initiation | Strain range (in %) |
|---|---|---|---|---|---|
| 1 | ±0.5r | $15^0$ | 5 | 2 | 0.6-0.65 |
| 2 | ±0.4r | 15 | 5 | 4 | 0.4-0.6 |
| 3 | ±0.3r | 15 | 5 | 5 | 0.3-0.4 |
| 4 | ±0.25r | 15 | 5 | 4 | 0.3-0.4 |

**Table 1.1.** The table shows the average results of five realizations of the simulated fiber configurations for each case. Four cases are shown, each with a different range of the radial and orientation variations.

| Realization | Without Voids | 10μm dia voids | 5μm dia voids | 2.5μm dia voids |
|---|---|---|---|---|
| 1 | 0.0035 | 0.0035 | 0.003 | 0.0035 |
| 2 | 0.0035 | 0.0055 | 0.004 | 0.0035 |
| 3 | 0.0035 | 0.0045 | 0.0035 | 0.0035 |
| 4 | 0.0035 | 0.0035 | 0.0035 | 0.0035 |
| 5 | 0.0035 | 0.0035 | 0.0035 | 0.0035 |

**Table 1.2.** The table shows the applied strain at which the dilatation energy density criterion is satisfied for fiber-matrix debonding to occur. Results for five realizations are shown for each case. The fiber distribution nonuniformity corresponds to the case 3 in Table 1.1, i.e., for ±0.3r and $\theta = 15^0$.

Table 1.2 shows the results corresponding to the presence of voids for the case when the radial variation of the fibers is in the range ±0.3r and the rotational movement of fibers is within $15^0$. Three different void sizes were studied, all simulating the situations with different degree of dispersion of voids within the composite. The largest voids will tend to be in the resin rich areas, while smaller voids will have higher probability of getting

into regions between fibers. As indicated in the table, for the smallest void size of 2.5 μm diameter, all five realizations showed no change in the strain for debonding initiation. As the void size is increased, the presence of voids affects (increases) the debonding strain. At the void size of 5.0 μm one out of five realization is affected, while two out of five realizations get increased debonding strain for 10.0 μm voids.

The fiber clustering decreases if during manufacturing the fibers are able to move more away from their initial positions in the dry bundle. With reduced fiber clusters the mode of failure initiation switches from debonding to yielding of the matrix. This is evidenced in Table 1.1 where for the least clustered case (±0.5r) only two out of five realizations show debonding. The corresponding strain shows doubling of the strain for debonding when compared to the most clustered case (±0.2r). When voids are introduced in the least clustered case, debonding becomes even more difficult to induce. The results obtained so far show that for ±0.4r, smaller voids that are able to find their way into the spaces between fibers reduce the tendency for debonding, while larger voids that get into the resin pockets have smaller effect on debonding.

In the **ongoing work**, the effects of large voids will be considered. Emphasis will be placed on voids that occupy regions between plies such as those seen in Fig. 1.1. These voids are expected to show effects on delaminations, in particular those that form due to diversion of ply cracks into the ply interfaces.

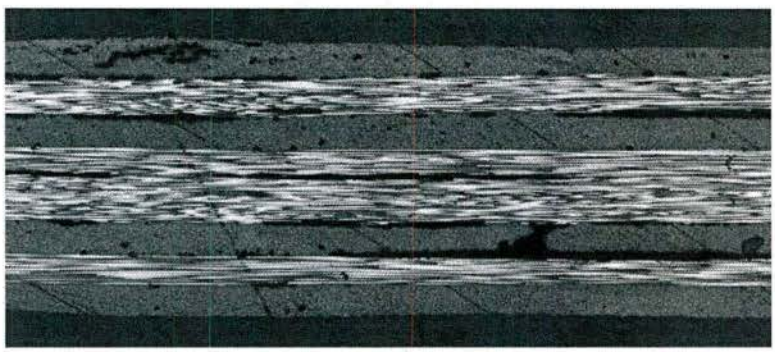

Fig. 1.1 An image of a composite laminate showing voids within the plies and between the plies. The voids within the plies are typically smaller and rounded, while those between the plies are larger and elongated.

**Task 2.2 Calibration of the Peridynamic model with SDM at the RVE-level**

**Background and motivation**

In order to calibrate the Peridynamic (PD) model to the RVE used in the SDM approach, we will re-create statistical PD models with exact geometry of fibers and matrix, and manufacturing defects present. An important problem that needs to be resolved in PD models is the stress oscillations that appear in the results because the nonlocal region

spans regions with different material properties at a sharp material interface. These oscillations are likely to influence the quasi-static and dynamic crack growth in the composite system. For this step we need a method that reduces/eliminates stress oscillations at an interface. A partially homogenized PD model has then to be calibrated and tested against the RVE results produced by the SDM formulation.

**Approach and Results**

In Peridynamics (PD), a material point interacts with every point around it within horizon. Near a surface/interface, a material's neighborhood is either not full or not of same phase and mechanical properties are not computed as intended unless something is modified. Taking the horizon to sufficiently small values for the effect to become negligible leads to a high computational cost. In problems with an inherent length-scale, the horizon size has to have a certain size. Here, we compare several approaches for correcting the surface effect. We introduce a PD model for better estimation of interfacial stress. A bimaterial sample is used to test the model against the classical solution. A two-phase composite sample with complex microstructure is used to observe differences between the original and the modified PD model.

**Surface and Interface effect in PD**

Consider, for example, the loading shown in the figure below (see Fig. 2.1). Near the boundaries, the PD solution differs from the classical solution because nodes near the boundaries have incomplete horizon regions and, if used without any changes, they employ the same bond properties computed for nodes with full horizon region in the bulk. The surface effect is also relevant in nonlocal formulations for modeling of material interfaces, and this is discussed below. In order to correct the surface effect, several methods have been proposed and we evaluated them.

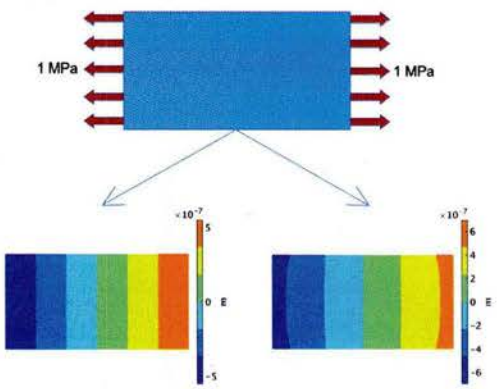


**Fig. 2.1**. Quasi-static stretching of an elastic material. Bottom row shows the horizontal displacement obtained with the classical model (analytical solution, left), and with the peridynamic model (right). Notice the surface effect present in the PD solution.

The results for comparing the maximum difference in horizontal and vertical discplacements between the various PD solutions and the classical one are shown in Fig.

2.2 below. While the fictitious node method gives the exact classical results, this method can only be applied for problems on simple geometries on in which no cracks form. For all other problems, the conclusion is that the volume correction method or the state-based formulation with no correction are the best options.

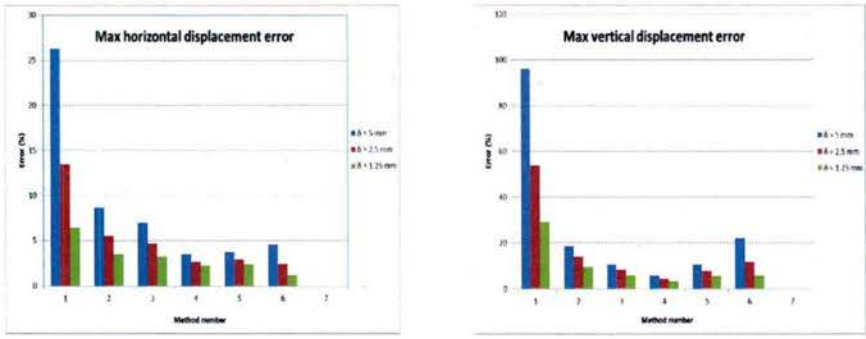


**Fig. 2.2**. The surface effect measured via differences for the maximum horizontal or vertical displacement in the sample between the classical solution and the PD solution with various methods of corrections and for different horizon sizes. The numbers on the horizontal axis mean: 1. Uncorrected bond based. 2. Uncorrected state based. 3. Volume correction method. 4. Force density correction method. 5. Energy correction method (bond based). 6. Energy correction method (state based). 7. Fictitious nodes method.

The effect of the precence of a material interface on the solution with a PD model is seen in Fig. 2.3 below. A two-phase material with a high constrast of elastic moduli is loaded under tension by applying loads horizontally. The problem is solved using quasi-static solver. While the classical model solution (obtained here using a fine FEM mesh) shows no sharp oscillations in the horizontal stress across the material interface, the PD solution with no corrections presents oscillations around this interface.

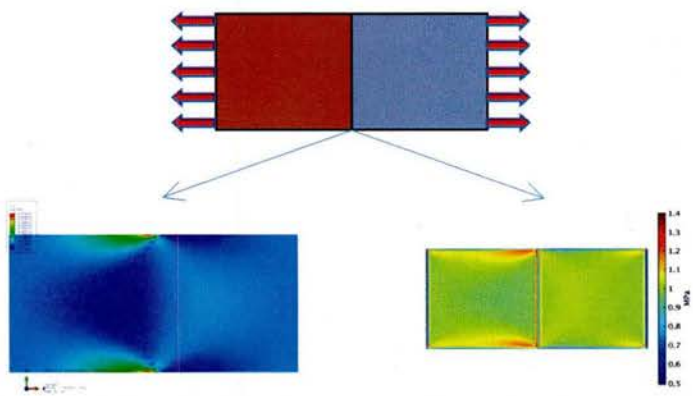

**Fig. 2.3**. The effect at a material interface measured via the horizontal stress in the sample. Left is the FEM result, on the right is the PD solution that presents oscillations at the material interface.

Using the volume average or the length average corrections methods eliminate the oscillations in the stress components (see Fig. 2.4 below). We find that the volume correction method is applicable in more general cases, including when the material interface is not a straight one, like in the case of fiber-reinforced composites.

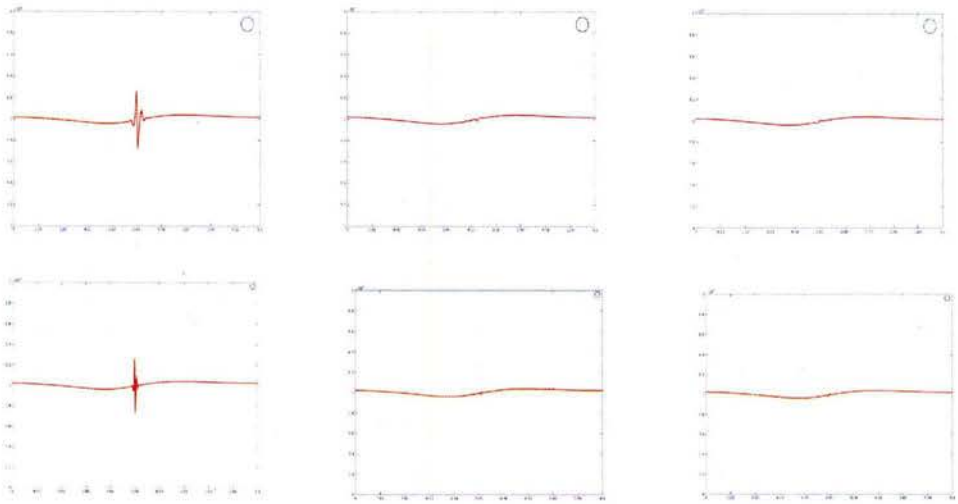

**Fig. 2.4**. Horizontal stress component along the horizontal midline of the sample shown in Fig. 2.3. The uncorrected (left column), and the corrected PD solutions with volume average method (center column) and volume average method (right column) for two different horizon sizes shown schematically in the top right corner of each figure, relative to the sample size dimension.